THE GJ 876 PLANETARY SYSTEM: A PROGRESS REPORT[1]

Gregory Laughlin,[2] R. Paul Butler,[3] Debra A. Fischer,[4] Geoffrey W. Marcy,[5]
Steven S. Vogt,[2] and Aaron S. Wolf[2]

ABSTRACT

We present an updated analysis of the GJ 876 planetary system based on an augmented data set that incorporates 65 new high-precision radial velocities obtained with the Keck Telescope from 2001 to 2004. These new radial velocities permit a more accurate characterization of the planet-planet interactions exhibited by the system. Self-consistent three-body orbital fits (which incorporate both the estimated instrumental uncertainties and Gaussian stellar jitter with $\sigma = 6$ m s^{-1}) continue to show that GJ 876 b (the outer planet of the system), and GJ 876 c (the inner planet of the system) are participating in a stable and symmetric 2:1 resonance condition in which the lowest order, eccentricity-type mean-motion resonance variables, $\theta_1 = \lambda_c - 2\lambda_b + \varpi_c$ and $\theta_2 = \lambda_c - 2\lambda_b + \varpi_b$, both librate around $0°$, with amplitudes $|\theta_1|_{\max} = 7°\!.0 \pm 1°\!.8$ and $|\theta_2|_{\max} = 34° \pm 12°$ (λ_b and λ_c are the mean longitudes, and ϖ_b and ϖ_c are the longitudes of periastron). The planets are also locked in a secular resonance, which causes them to librate about apsidal alignment with $|\varpi_1 - \varpi_2|_{\max} = 34° \pm 12°$. The joint line of apsides for the system is precessing at a rate $\dot{\varpi} \sim -41°$ yr^{-1}. The small libration widths of all three resonances likely point to a dissipative history of differential migration for the two planets in the system. Three-body fits to the radial velocity data set, combined with a Monte Carlo analysis of synthetic data sets, indicate that the (assumed) coplanar inclination, i_s, of the system is $i_s > 20°$. Configurations with modest mutual inclination are, however, also consistent with the current radial velocity data. For non-coplanar configurations, the line of nodes of the inner planet precesses at rates of order $-4°$ yr^{-1}, and in these cases, the inner planet can be observed to transit the parent star when either the ascending or descending node precesses through the line of sight. Therefore, GJ 876 c may possibly be observed to transit in the relatively near future even if it is not transiting at the present time. We comment briefly on the orbital stability of as-yet-undetected terrestrial planets in habitable orbits and assess the suitability of the system as a potential target for upcoming space missions such as the *Terrestrial Planet Finder*.

Subject headings: planetary systems — planets and satellites: general — stars: individual (GJ 876)

Online material: color figure

1. INTRODUCTION

GJ 876 (HIP 113020) is the lowest mass star currently known to harbor planets, and it is accompanied by perhaps the most remarkable exoplanetary system discovered to date. In 1998, Marcy et al. (1998) and Delfosse et al. (1998) announced the discovery of a $P \sim 60$ days companion orbiting the star. This planet, designated GJ 876 b is a super-Jovian object, with $M \sin(i) = 1.9 M_J$, and it induces a large ($K \sim 210$ m s^{-1}) radial velocity variation in its red dwarf companion. After continued Doppler monitoring of GJ 876, Marcy et al. (2001) announced the discovery of a second [$M \sin(i) = 0.6 M_J$] planet in the system. This object (designated GJ 876 c) has a $P \sim 30$ days orbit, and was identified to be participating in a 2:1 mean-motion resonance with the outer planet b.

The red dwarf GJ 876 (R.A. $= 22^h5^m$, decl. $= 14°16'$) is observable from both hemispheres and is distinguished by being the fortieth nearest stellar system, with a *Hipparcos*-determined distance of 4.69 pc (Perryman et al. 1997). Its spectral type is M4 V. Using the bolometric correction of Delfosse et al. (1998), the *Hipparcos*-estimated parallax indicates a stellar luminosity of 0.0124 $L_\odot$. The red dwarf mass-luminosity relation of Henry & McCarthy (1993) therefore implies a mass of 0.32 $M_\odot$ and an estimated radius of $R_* = 0.3$ $R_\odot$.

A definitive identification of the resonance conditions obeyed by the planets is made possible by the large dynamic range of the GJ 876 radial velocities. Among the 113 Doppler velocities obtained with the Keck Telescope, the individually estimated instrumental errors have an average precision of 4.65 m s^{-1}, with individual precision estimates ranging as low as 2.3 m s^{-1}. The two planets induce velocity swings in the star of nearly 0.5 km s^{-1} and thus allow us to take full advantage of the fine Doppler precision. Furthermore, the outer planet has been observed for more than 40 orbital periods. These fortuitous circumstances allow the planet-planet interactions to be probed with a degree of refinement that is exceeded only for the planets in the solar system (e.g., Laplace 1799–1802) and by the planets orbiting the 6.2 ms radio pulsar PSR B 1257+12 (Wolszczan & Frail 1992; Konacki & Wolszczan 2003).

The gravitational perturbations exerted by the planets on each other induce a significant non-Keplerian component to the orbital motion. In particular, the periastra of the planets precess at a rate $\dot{\varpi} \sim -41°$ yr^{-1}. The non-Keplerian aspects of the motion lead to a relatively high best-fit value (currently $\sqrt{\chi^2} = 2.81$) for models that use dual-Keplerian fitting functions to model the observed radial velocity variation. The strong planet-planet perturbations do, however, enable the construction of

[2] UCO/Lick Observatory, University of California at Santa Cruz, Santa Cruz, CA 95064; laughlin@ucolick.org.
[3] Department of Terrestrial Magnetism, Carnegie Institution of Washington, 5241 Broad Branch Road Northwest, Washington DC, 20015-1305.
[4] Department of Physics and Astronomy, San Francisco State University, San Francisco, CA 94132.
[5] Department of Astronomy, University of California, Berkeley, CA 94720.

TABLE 1
Measured Velocities for GJ 876 (Keck)

JD (−2,440,000)	Radial Velocity (m s⁻¹)	Uncertainty (m s⁻¹)
10,602.093	275.000	4.83744
10,603.108	293.541	4.87634
10,604.118	283.094	4.67169
10,605.110	280.726	5.52761
10,606.111	263.544	4.98461
10,607.085	233.736	4.69071
10,609.116	150.489	5.45623
10,666.050	280.291	5.21384
10,690.007	−166.391	5.10688
10,715.965	143.299	4.61302
10,785.704	311.515	8.24044
10,983.046	−105.733	4.95257
10,984.094	−123.184	5.06684
11,010.045	−94.0837	4.60856
11,011.102	−73.0974	3.64249
11,011.986	−45.1522	2.97916
11,013.089	−18.1096	5.04988
11,013.965	1.82459	3.41393
11,043.020	−88.9192	4.74611
11,044.000	−115.336	4.14800
11,050.928	−159.471	4.70908
11,052.003	−144.716	5.26416
11,068.877	−132.122	4.85189
11,069.984	−103.148	4.23548
11,070.966	−109.364	4.57718
11,071.878	−78.1619	4.73338
11,072.938	−62.7263	4.78583
11,170.704	−125.859	6.25166
11,171.692	−134.732	6.13061
11,172.703	−114.607	5.41503
11,173.701	−110.987	6.15440
11,312.127	−145.816	4.74986
11,313.117	−147.122	5.23696
11,343.041	30.2319	4.84609
11,368.001	−194.527	4.32588
11,369.002	−198.763	4.71886
11,370.060	−178.623	4.44845
11,372.059	−175.318	8.09112
11,409.987	−92.8259	4.43375
11,410.949	−92.9346	4.29902
11,411.922	−105.284	4.83919
11,438.802	−72.3787	4.40473
11,543.702	−155.604	6.97488
11,550.702	−195.472	6.43277
11,704.103	107.247	4.76474
11,706.108	60.9448	5.38786
11,755.980	251.808	7.45259
11,757.038	233.575	5.95792
11,792.822	−220.933	4.59942
11,883.725	171.247	5.53578
11,897.682	39.5285	6.05218
11,898.706	37.9805	5.67651
11,899.724	27.5835	6.14660
11900.704	11.2978	5.16144
12,063.099	197.931	5.85069
12,095.024	−242.481	5.64944
12,098.051	−281.799	5.68766
12,099.095	−267.919	5.08161
12,100.066	−275.558	5.42508
12,101.991	−254.637	5.08017
12,128.915	122.199	6.13512
12,133.018	55.8623	5.23130
12,133.882	59.7818	5.75232
12,160.896	−256.467	5.11438

TABLE 1—*Continued*

JD (−2,440,000)	Radial Velocity (m s⁻¹)	Uncertainty (m s⁻¹)
12,161.862	−269.742	5.63196
12,162.880	−237.342	5.50410
12,188.909	95.7486	5.98643
12,189.808	99.2101	6.39510
12,236.694	164.781	6.22869
12,238.696	187.889	5.50345
12,242.713	197.089	6.73589
12,446.071	75.3063	6.21285
12,486.917	185.162	3.98475
12,487.124	174.897	3.63466
12,487.919	171.914	4.32865
12,488.127	170.714	3.83680
12,488.945	149.798	2.28548
12,514.867	−129.741	5.24131
12,515.873	−156.261	4.97779
12,535.774	32.8722	5.56979
12,536.024	41.7095	5.54259
12,536.804	74.7051	6.10848
12,537.013	66.7469	4.94657
12,537.812	76.0011	5.38256
12,538.014	83.6270	5.03001
12,538.801	107.662	4.73423
12,539.921	123.450	5.36501
12,572.713	−43.1787	4.71435
12,572.919	−53.0618	5.07898
12,573.742	−66.6653	4.44116
12,573.878	−73.8528	4.31492
12,574.763	−112.285	4.29373
12,574.940	−116.120	4.66948
12,575.719	−136.679	4.42299
12,600.751	118.311	3.86951
12,601.750	125.363	3.89455
12,602.721	147.247	4.25502
12,651.718	−129.194	8.13000
12,807.028	148.787	5.36857
12,829.008	−254.556	4.39146
12,832.080	−180.797	4.86352
12,833.963	−135.235	4.79979
12,835.085	−100.468	4.85671
12,848.999	141.070	6.62912
12,850.001	127.450	6.13066
12,851.057	121.834	5.86209
12,854.007	84.0791	5.10877
12,856.016	112.441	5.21600
12,897.826	−55.1842	4.93230
12,898.815	−26.9680	4.83134
12,924.795	215.024	5.67363
12,987.716	198.162	7.74271
12,988.724	194.946	5.98031

dynamical fits to the radial velocity data that both improve the $\sqrt{\chi^2}$ statistic of the orbital fit and place the planets into the secular apsidal alignment resonance and deeply within the two coplanar 2:1 mean-motion resonances (Laughlin & Chambers 2001; Rivera & Lissauer 2001; Nauenberg 2002). The existence of this multiply resonant configuration can be understood as the consequence of differential migration of the two planets within GJ 876's protoplanetary disk (e.g., Lee & Peale 2001, 2002; Lee 2004), and the presence of strong mutual interactions between the two planets leads to a partial removal of the so-called sin *i* degeneracy. System configurations in which the planetary orbits are inclined by less than 30° to the plane of the sky exhibit significantly worse fits to the radial velocity data.

TABLE 2
COPLANAR FIT TO GJ 876 RADIAL VELOCITY DATA

Parameter	Planet c	Planet b
P (days)......................	30.38 ± 0.03	60.93 ± 0.03
M (deg).......................	0 ± 15	186 ± 13
e...................................	0.218 ± 0.002	0.029 ± 0.005
i fixed (deg)	90.0	90.0
ϖ (deg)......................	154.4 ± 2.9	149.1 ± 13.4
m (M_J)	0.597 ± 0.008	1.90 ± 0.01
o_1 m s^{-1}	-8.732	...
o_2 m s^{-1}	44.476	...
Transit epoch..............	JD $2,453,000.57 \pm 0.22$	...
$|\varpi_c - \varpi_b|_{max}$ (deg).......	34 ± 11	...
θ_{1max} (deg).................	7.0 ± 1.8	...
θ_{2max} (deg).................	34 ± 12	...
Epoch	JD $2,449,679.6316$	...

The importance of the GJ 876 system arises because it can provide interesting constraints for theories of planetary formation. Because the current resonant state is sensitive to details of the system's history, it is worthwhile to evaluate the degree of confidence that can be placed in the present best-fit orbital parameters. The plan of this short paper is thus as follows: In § 2 we describe coplanar fits to the radial velocity data set. These fits allow us to construct a detailed model of the system, and equally importantly, allow us to evaluate the confidence for which we can determine the orbital parameters. In § 3 we broaden our analysis to include the possibility of system configurations in which the planets do not orbit in the same plane. In this case, the orbital angular momentum vectors of the planets can precess and the planets can be potentially observed to evolve through transiting configurations. In § 4 we briefly discuss how our results bear on current theoretical studies of the nascent GJ 876 planetary system.

2. COPLANAR CONFIGURATIONS OF THE TWO PLANETS

We first assume that the planets GJ 876 b and c are in a coplanar configuration perpendicular to the plane of the sky ($i_s = i_b = i_c = 90°$) and obtain self-consistent three-body fits to the combined Lick-Keck radial velocity data set. This set includes the 16 Lick velocities listed in Marcy et al. (2001) and the 113 Keck velocities listed in Table 1. All of our orbital fits are obtained using a Levenberg-Marquardt multiparameter minimization algorithm (Press et al. 1992) driving a three-body integrator as described in Laughlin & Chambers (2001). The best edge-on coplanar fit is listed in Tables 2 and 3. This reference fit has 12 free parameters, including the planetary periods, P_b and P_c; the mean anomalies, M_b and M_c at epoch JD 2449679.6316; the orbital eccentricities, e_b and e_c; the

longitudes of periapse, ϖ_b and ϖ_c; the planetary masses, m_b and m_c; and two velocity offsets, o_1 and o_2. The quantity o_1 is an offset velocity added to the first GJ 876 radial velocity, v_{L1}, obtained with the Lick 3 m telescope ($t =$ JD 2, 449, 679.6316, $v_{L1} = 58.07$ m s^{-1}; see Marcy et al. 2001). The parameter o_2 is an offset velocity added to all of the radial velocities taken with the Lick Telescope. It accommodates the different velocity zero points of the Lick and Keck Telescopes. The mass of the star is fixed at 0.32 $M_\odot$. The mean longitudes, λ_i (used to compute the mean-motion resonant arguments), are related to the mean anomalies and longitudes of periapse through $\lambda_i = \varpi_i + M_i$.

The orbital elements listed in Table 2 are osculating orbital elements at epoch JD 2449679.6316 (the epoch of the first radial velocity point taken at Lick Observatory in 1994.9 listed by Marcy et al. 2001) and are expressed in Jacobi coordinates. As explained in Rivera & Lissauer 2001 and Lee & Peale 2003, Jacobi coordinates are the most natural system for expressing multiple-planet fits to radial velocity data. For reference, in Table 3 we express the orbital configuration of the system (again at JD 2449679.6316) in Cartesian coordinates. In the Cartesian system, the line of sight from the Earth to the star is in the negative y-direction and the y-component of velocity for the star relative to the system center of mass is measured, by convention, as a negative radial velocity.

The uncertainties in the orbital fit are estimated using Monte Carlo simulation of synthetic data sets (Press et al. 1992). In this procedure, we assume that the true configuration of the system is that given by the orbital parameters listed in Tables 2 and 3 (i.e., the best-fit coplanar, edge-on system). We produce 100 synthetic data sets by integrating this assumed planetary configuration forward in time, sampling the stellar reflex velocity at all of the observed epochs and adding (in quadrature) noise drawn from Gaussian distributions corresponding to (1) an assumed $\sigma = 6$ m s^{-1} stellar jitter and (2) the individual velocity errors. Chromospherically quiet G and K dwarfs in the ongoing radial velocity surveys typically show rms scatters $\sigma \sim 3-5$ m s^{-1} arising from stellar jitter (Saar et al. 1998). Nauenberg (2002) argued that excess scatter in the dynamical fits to the GJ 876 radial velocity data should be attributed to a stellar jitter of 2–4 m s^{-1}. Preliminary work by J. Wright & G. W. Marcy (2005, in preparation) indicates that M3–M4 dwarfs with chromospheric activity similar to GJ 876 display typical jitter values $\sigma = 4 \pm 2$ m s^{-1}, motivating our conservative choice of $\sigma = 6$ m s^{-1}.

The assumption of a 6 m s^{-1} stellar jitter gives an average $\sqrt{\chi^2} = 1.51 \pm 0.09$ for the fits to the synthetic data sets, consistent with the value $\sqrt{\chi^2} = 1.535$ obtained from fitting to the actual data set. (All the $\sqrt{\chi^2}$ values that we quote are computed using only the instrumental uncertainties, and they do not include the scatter expected to arise from stellar jitter.) The uncertainty quoted for each orbital parameter is the variance computed for the parameter from the fits to the 100 synthetic

TABLE 3
BARYCENTRIC CARTESIAN INITIAL CONDITIONS FOR COPLANAR FIT TO GJ 876 RADIAL VELOCITY DATA

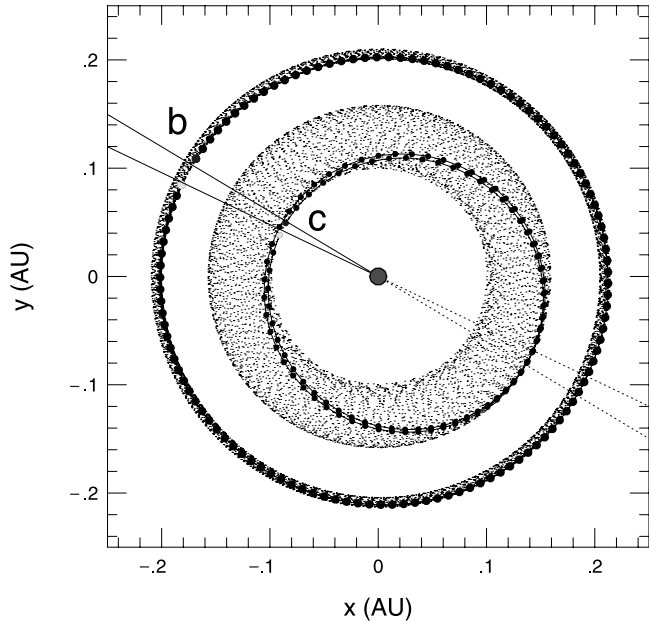| Parameter	Star	Planet c	Planet b
Mass (gm)	$6.36515181 \times 10^{32}$	$1.13341374 \times 10^{30}$	$3.59700414 \times 10^{30}$
x (cm).....................................	0.0	$-1.3739370 \times 10^{12}$	$2.89833447 \times 10^{12}$
y (cm).....................................	0.0	6.6185776×10^{11}	$-1.3485766 \times 10^{12}$
z (cm)	0.0	0.0	0.0
v_x cm s^{-1}	-3.97415664×10^3	-2.53217478×10^6	1.50114165×10^6
v_y cm s^{-1}	-9.01247643×10^3	-5.26220995×10^6	3.25294014×10^6
v_z cm s^{-1}	0.0	0.0	0.0

FIG. 1.—Orbital motion arising from the two-planet coplanar dynamical fit to the GJ 876 system listed in Tables 2 and 3. The clouds of small black dots plot the positions of the planets at every one-half day interval from JD 2,449,680 to JD 2,453,000, illustrating the range of planetary motion produced by the precession of the line of apsides. The connected filled circles plot the positions of the planets at 120 one-half day intervals beginning on JD 2,449,710. The two solid lines radiating from the central star mark the osculating longitudes of periastron, $\varpi_b = 149°.1$ and $\varpi_c = 154°.4$ for the planets at JD 2,449,710. The longitudes ϖ_b and ϖ_c oscillate about alignment with a libration amplitude $|\varpi_c - \varpi_b|_{\max} = 34°$, and the line of apsides precesses at a rate $\dot\varpi = -41°$ yr^{-1}. The sense of the orbital motion is counterclockwise as viewed from above. [*See the electronic edition of the Journal for a color version of this figure.*]

data sets. We find that the distributions of parameter estimates are generally consistent with underlying Gaussian distributions. We note, however, that significant covariation does exist between some of the orbital parameters (e.g., M_i and ϖ_i), making it impossible to generate systems that are fully consistent with the radial velocity data by independently sampling orbital parameters from the inferred underlying distributions.

We conclude that the nominal, edge-on, coplanar two-planet model of Table 2 is fully consistent with the current set of radial velocity measurements of the star. If the actual stellar jitter for GJ 876 is smaller than 6 m s^{-1}, then one can contemplate extracting additional information (related, say, to the inclinations and nodes of planets b and c, or to additional bodies) from the lists of radial velocities in Table 1 and in Marcy et al. (2001).

The three-body fit to the radial velocities indicates that the two major planets in the GJ 876 are locked in a symmetric configuration, with the resonant arguments $\theta_1 = \lambda_c - 2\lambda_b + \varpi_c$, and $\theta_2 = \lambda_c - 2\lambda_b + \varpi_b$ both librating about zero degrees. The orbital configuration of the best-fit edge-on coplanar model of the GJ 876 data set is shown in Figure 1. In this figure, the positions of the planets are plotted as filled circles at 60 successive one-half-day intervals beginning on JD 2,449,710, when the planets were both near periastron. The positions are plotted in the frame centered on the star. Also plotted (as clouds of dots) are the positions of the planets at every one-half-day interval since the epoch of the first Lick Observatory data point taken on JD 2,449,679.6316. The figure shows that the orbits of the planets do not close, while examination of the time-dependent osculating orbital elements shows that the periapses of the planets are precessing at a rate of $\dot\varpi = -41°$ yr^{-1}. This rapid precession is the primary reason
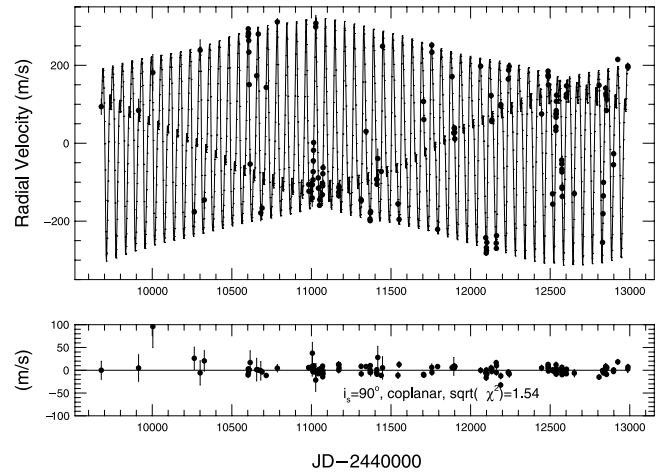

FIG. 2.—*Top:* Stellar reflex velocity from a self-consistent, coplanar, $i_s = 90°$ three-body integration compared to the GJ 876 radial velocities. The fit parameters and initial conditions for the integration are listed in Tables 2 and 3. Velocities obtained at Lick Observatory (listed in Marcy et al. 2001) and the velocities taken at Keck Observatory (listed in Table 1) are shown as small filled circles. The plotted Lick velocities include a fitted offset between the telescopes that resulted in $o_2 = 44.476$ m s^{-1} being added to each of the 16 Lick Observatory measurements. *Bottom:* Residuals to the orbital fit.

why Keplerian fits to the data show higher $\sqrt{\chi^2}$ values than the self-consistent three-body fits.

Figure 2 shows the fitted reflex velocity of the star in comparison with the radial velocity data. The most striking feature of this figure (aside from the dominant $\sim$60 days periodicity) is the modulation arising from the 8.7 yr precession period for the planets' joint line of apsides. This precession has now been observed for more than one full period, and the planets have completed a full librational cycle for both the secular $|\varpi_c - \varpi_b|$ resonance argument, as well as the 2:1 resonance arguments θ_1 and θ_2. These librations are manifest in the slightly non-sinusoidal envelope of the overall stellar reflex velocity. The non-Keplerian aspect of the motion is also evident in the wave of small-amplitude velocity reversals running through the radial velocity curve. In the summed Keplerian model, this wave has an asymmetric shape and is produced (along with the overall modulation) by the inner planet c having a fixed period $P_c = 30.12$ days that is slightly less than half the $P_b = 61.02$ days period of the outer planet. In the self-consistent fit, the small velocity reversals display a symmetric waveform, and arise largely from the precession of the inner eccentric orbit and the librations about the three resonances. For additional related discussion of the manifestation of the orbital dynamics in the radial velocity curve, see Nauenberg (2002)

The primary assumption underlying the fit given in Tables 2 and 3 is that the planetary orbits are coplanar and are being viewed edge-on. While there is no a priori observational evidence to indicate that the system is coplanar, it is likely that the planets arose from a relatively flat protoplanetary accretion disk. Numerical integrations of the differential migration of the system that assume this scenario show that the eccentricity must in general be forced to higher values than observed before significant mutual inclination is excited (see also Thommes & Lissauer 2003). Hence it makes dynamical sense to prefer coplanar models. We also note that astrometric evidence obtained by Benedict et al. (2002) suggests that the outer planet in the system is being viewed fairly close to an edge-on configuration.

If we assume coplanar inclinations with $i_s < 90°$ and construct a succession of fits, we obtain the run of best-fit $\sqrt{\chi^2}$
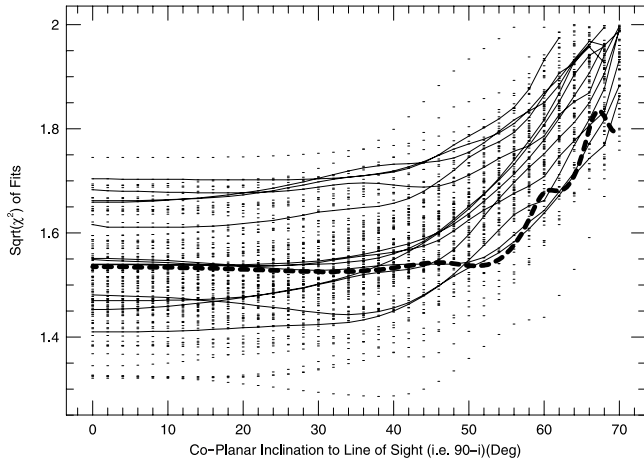
FIG. 3.—Values of $\sqrt{\chi^2}$ obtained from three-body fits to the GJ 876 radial velocity data as a function of coplanar inclination, $90 - i$ (*thick dashed line*). Also shown are the $\sqrt{\chi^2}$ values obtained (as a function of assumed coplanar inclination) from fits to Monte Carlo realizations of the edge-on configuration listed in Table 2 (*black lines and cloud of black dots*).

FIG. 5.—Maximum libration angle $|\varpi_c - \varpi_b|_{max}$ observed in fits to the GJ 876 radial velocity data (*thick dashed line*), along with fits to Monte Carlo realizations of the edge-on configuration listed in Table 2 (*black lines and cloud of black dots*).

values shown by the thick dashed line of Figure 3. This sequence shows a very slight decline in the value of $\sqrt{\chi^2}$ as the system is tilted from $i_s = 90°$ ($\sqrt{\chi^2} = 1.535$) to $i_s = 59°$ ($\sqrt{\chi^2} = 1.525$). For coplanar inclinations having $i_s < 38°$, however, $\sqrt{\chi^2}$ experiences a rapid rise. Similar behavior in the $\sqrt{\chi^2}$ profile was observed by both Laughlin & Chambers (2001) and Rivera & Lissauer (2001), although with more radial velocity data, the dip in $\sqrt{\chi^2}$ has grown shallower. Laughlin & Chambers (2001) and Rivera & Lissauer (2001) both interpreted the configuration with the minimum $\sqrt{\chi^2}$ as representing the likely coplanar inclination of the system, whereas Nauenberg (2002) suggested that the improvement found by those authors in going from $i_s = 90°$ to $i_s \sim 45°$ was not significant. Our primary aim is thus to ascertain what significance can be ascribed to this trend in $\sqrt{\chi^2}$. That is, which coplanar inclinations can be ruled out by the dynamical fits to the data?

In Figure 4 we plot the best-fit osculating eccentricities, e_b and e_c, as a function of coplanar inclination $90 - i_s$. As i_s decreases from $90°$, the fitted planetary masses increase by $\sin i$, and the fitted eccentricities also increase. The inner planet

eccentricity, for example, increases from $e_c = 0.22$ at $i_s = 90°$ to $e_c = 0.38$ at $i_s = 20°$. The best-fit $\sqrt{\chi^2}$ value, however, changes very little in the face of this large eccentricity increase. This behavior occurs because the primary non-Keplerian interaction between the planets is the $\dot{\varpi} = -41°$ yr^{-1} precession (see, e.g., Ford 2003). As the masses of the planets increase, the precession rate also increases. This increase, however, can be essentially exactly offset by an increase in the orbital eccentricities, which act to decrease $\dot{\varpi}$.

For each of the 100 Monte Carlo realizations of synthetic data sets that were previously generated for the edge-on coplanar system listed in Tables 2 and 3, we perform the same procedure of incrementing the coplanar inclination and obtaining fits. The results are shown as the cloud of dots in Figure 3, in which 13 randomly selected sequences are also plotted as dark lines in order to give a representative idea of the trends for particular realizations. These fits show that the shallow minimum observed near $i \sim 60°$ in the fits to the actual data cannot be believed.

Figures 5, 6, and 7 show the fitted values of the 2:1 and secular libration widths ($|\theta_1|_{max}$, $|\theta_2|_{max}$, and $|\varpi_b - \varpi_c|_{max}$)
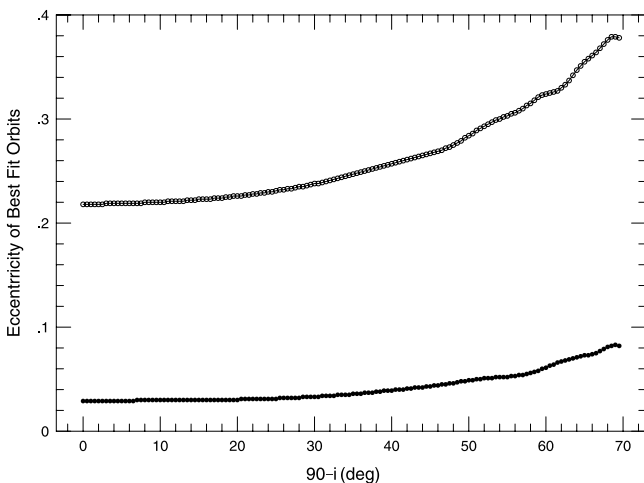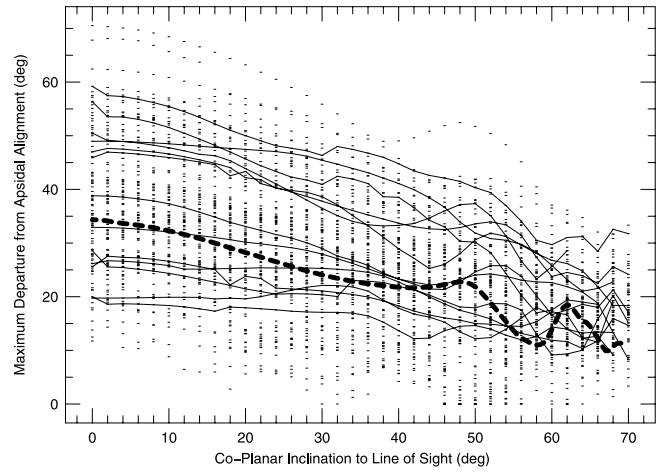

FIG. 4.—Eccentricity of the inner planet, e_c (*connected open symbols*) and the outer planet, e_b (*connected filled symbols*) vs. $\sin i$ for coplanar two-planet fits to the GJ 876 radial velocity data set.
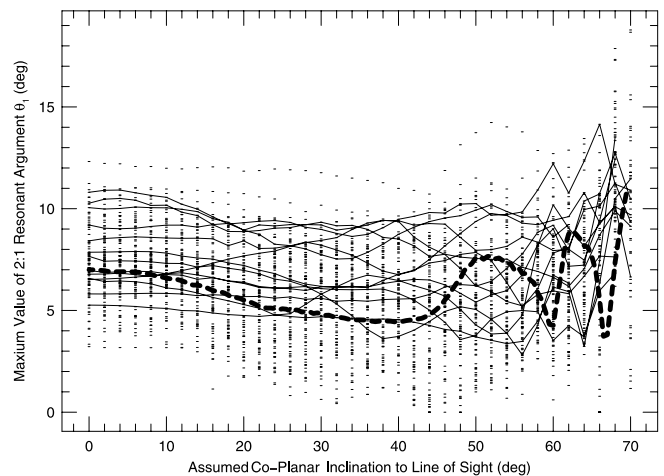

FIG. 6.—Maximum libration of the 2:1 resonant argument $|\theta_1|_{max}$ observed in fits to the GJ 876 radial velocity data (*thick dashed line*), along with fits to Monte Carlo realizations of the edge-on configuration listed in Table 2 (*black lines and cloud of black dots*).
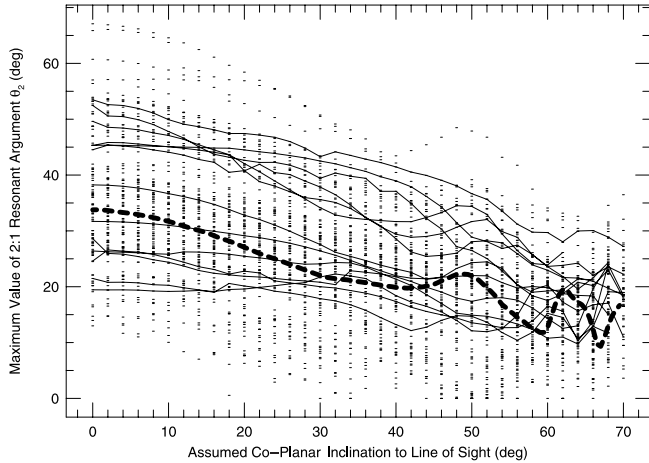
FIG. 7.—Maximum libration of the 2:1 resonant argument $|\theta_2|_{max}$ observed in fits to the GJ 876 radial velocity data (*thick dashed line*), along with fits to Monte Carlo realizations of the edge-on configuration listed in Table 2 (*black lines and cloud of black dots*).

as a function of coplanar inclination for the Monte Carlo realizations. The fits to the actual data (*thick dashed lines*) are fully consistent with the behavior observed in the Monte Carlo realizations, providing further evidence that the inclination of the coplanar system cannot be confidently extracted from the data (assuming Gaussian stellar jitter with $\sigma = 6$ m s^{-1}).

The libration width figures indicate that as the masses of the planets are increased (i.e., as $90 - i_s$ increases) the libration widths $|\theta_1|_{max}$, $|\theta_2|_{max}$, and $|\varpi_b - \varpi_c|_{max}$ all show a decrease, reaching minimum values near $i_s \sim 45°$. This phenomenon occurs because the librations are more readily sensed in a radial velocity data set for planets of larger mass. Hence, a given observed perturbation must arise from a smaller libration if the planet masses are increased. The increase in $\sqrt{\chi^2}$ observed for systems with $i_s < 30°$ is associated with the inability to match the observed perturbations with further decreases in the libration widths of the resonances. We note that simulations of resonant capture (Kley et al. 2004) and differential migration favor narrow libration widths. These scenarios would therefore favor the prediction that the system will eventually be found to lie in the neighborhood of $i_s \sim 45°$.

3. THE PROSPECTS FOR OBSERVING GJ 876 c IN TRANSIT

The a priori probability that a planet on a Keplerian orbit transits its parent star as seen from the line of sight to Earth is given by

$$\mathcal{P}_{transit} = 0.0045 \left(\frac{1 \text{ AU}}{a}\right) \left(\frac{R_* + R_{pl}}{R_\odot}\right) \left[\frac{1 + e \cos(\pi/2 - \varpi)}{1 - e^2}\right],$$

(1)

where a is the semimajor axis of the orbit, R_* and R_{pl} are the radii of the star and planet, respectively, e is the orbital eccentricity, and ϖ is the argument of periastron referenced to the intersection of the plane of the sky with the orbital plane, namely, the line of nodes. For the inner planet of the GJ 876 system, this probability is only $\sim 1\%$ if we assume a stellar radius of $R = 0.3\ R_\odot$. Planet-planet interactions in the GJ 876 system, however, allow the nodal line of the inner, less massive planet to precess into transit for a significantly wider variety of

observationally consistent non-coplanar configurations. Transits of GJ 876 by the inner planet c, if they occur, are therefore likely to be visible for a period of order 2 yr as the node of the planetary orbit sweeps across the face of the star. The scientific opportunities from such transits would be somewhat analogous to the opportunities provided by the series of mutual eclipses observed in the Pluto-Charon system in the 1980s (Binzel 1989). Such configurations require a mutual inclination between planets b and c. Because a transiting configuration is relatively easy to observe (the transit depth is expected to be of order 10%, this system makes an interesting photometric target for small-aperture telescopes (e.g., Seagroves et al. 2003).

Using the planetary evolution models computed by Bodenheimer et al. (2003) and assuming $i_s = 90°$, we estimate that the planetary radius of GJ 876 c should be $0.93R_J$ if the planet has a solid core and $1.03R_J$ if it does not. Insolation-driven atmospheric-interior coupling, which can lead to an increased radius (see, e.g., Guillot & Showman 2002), is expected to be negligible for planet c. For an assumed tidal quality factor $Q = 10^6$, the eccentricity damping timescale is of order 250 Gyr (Goldreich & Soter 1966), indicating that the energy generated by interior tidal heating should not affect the planetary radius. We estimate that the effective temperature at the planet's $\tau = 1$ surface is 210 K, assuming an albedo $a = 0.4$.

Benedict et al. (2002) used the fine guidance sensor instrument on *Hubble Space Telescope* to obtain a preliminary measurement of the inclination of the outer planet in the GJ 876 system, obtaining a value $i_b = 84° \pm 6°$. In order to illustrate the possibility that the inner planet may periodically experience transit epochs, we assume that the orbital plane of the outer planet is coincident with the line of sight at JD 2,449,679.6316 ($i_b = 90°$). We then choose (1) a specific value for the osculating inclination of the inner planet at the epoch of the first radial velocity point, as well as (2) the osculating value of the difference in nodal longitudes at the first radial velocity epoch. With these parameters fixed, we then obtain a self-consistent fit to the radial velocity data to determine all the other orbital parameters. When an acceptable fit is obtained, we integrate the system forward to check for the occurrence of (inner planet) transits within the next 100 yr.

The results are shown in the lower left-hand panel of Figure 8, which shows the result of 1296 such separate self-consistent fits. In the figure, the fits are organized by the choice of osculating starting inclination of the inner planet orbit (y-axis of the figure panels) and by the initial angle between the two ascending nodes (x-axis of the figure panels). The nominal edge-on coplanar system therefore corresponds to the bottom row of cells. Scenarios where the inner planet was transiting during the last season of observations (and specifically during the transit epoch near JD 2,453,000.57) have their cells colored black. Systems that start transiting within 100 yr of the last radial velocity observation in Table 1 are indicated by dark gray (transits to start very soon) to light gray (transits starting in the year 2103). Some regions of the diagram contain systems that were transiting during the past 10 yr but that have by now moved out of alignment. On average, over the range of configurations plotted in Figure 8, the line of nodes of the inner planet precesses at rates of order $-4°$ yr^{-1}.

The lower right-panel of Figure 8 maps the distribution of $\sqrt{\chi^2}$ values obtained for the 1296 separate self-consistent fits. The lowest values found are $\sqrt{\chi^2} = 1.52$, matching the best-fit coplanar $i_s = 90°$ model. All of the models have $\sqrt{\chi^2} < 1.65$. The Monte Carlo analysis of the previous section thus indicates that they are acceptable fits to the radial velocity data, assuming $\sigma = 6$ m s^{-1}. In the top two panels of Figure 8, we plot
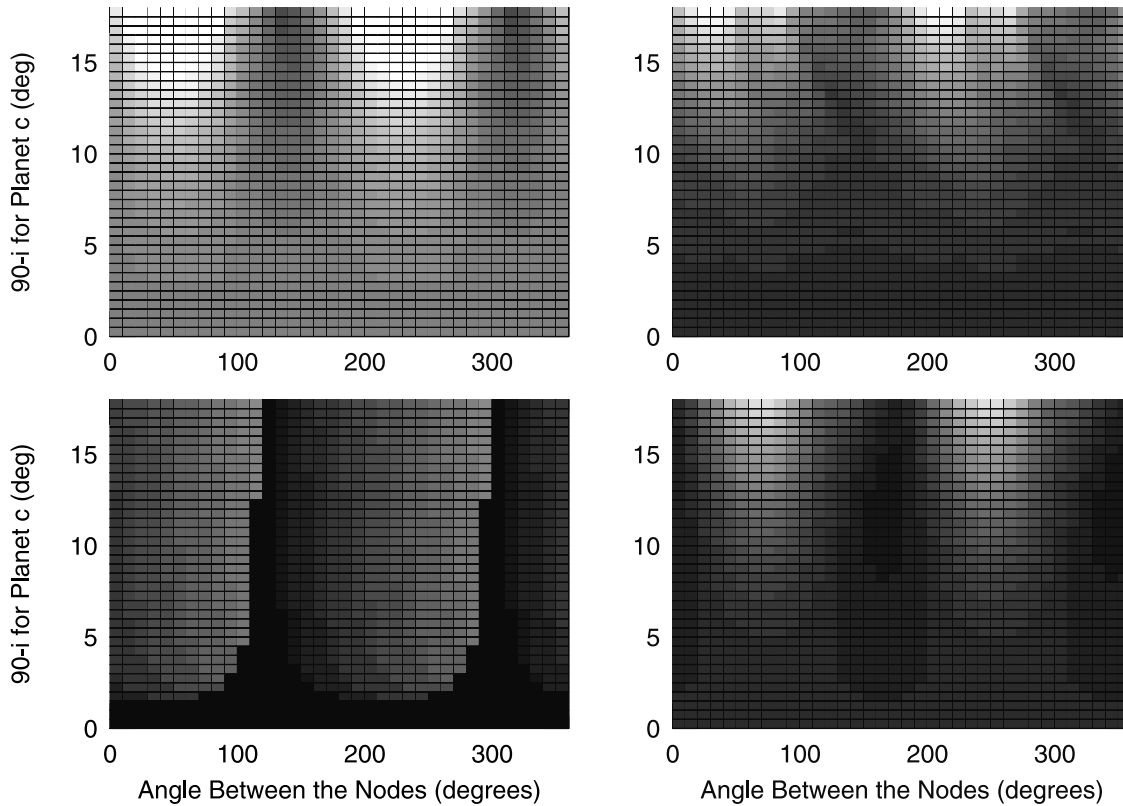
FIG. 8.—*Upper left panel*: $|\varpi_c - \varpi_b|_{\max}$ for fits in which the two planets are assumed to be mutually inclined. For all fits, $i_b = 90°$ at epoch JD 2,449,679.6316. Fits are gridded according to $\Omega_c - \Omega_b$ (*x*-axis of each panel) and $90° - i_c$ (*y*-axis of each panel). The grid cell corresponding to each fit is color coded and can vary from white ($|\varpi_c - \varpi_b|_{\max} \geq 60°$) to dark ($|\varpi_c - \varpi_b|_{\max} \leq 10°$). *Upper right panel*: Same as upper left panel, except $\theta_{1\max}$ is plotted with color coding ranging from white ($\theta_{1\max} \geq 20°$) to dark ($\theta_{1\max} \leq 5°$). *Lower right panel:* Same as upper left panel, except $\sqrt{\chi^2}$ is plotted for each fit with color coding ranging from white ($\sqrt{\chi^2} \geq 1.65$) to dark ($\sqrt{\chi^2} \leq 1.52$). *Lower left panel:* Same as upper left panel, except the starting epochs for transits of planet c are plotted for each fit with color coding ranging from light gray (transits in year 2100), to dark (transiting during the first line of sight passage after epoch JD 2,452,988.724 of the last radial velocity measurement in Table 1).

the libration widths of the secular apsidal alignment and the θ_1 resonance argument for each fit. These panels show that, for the range of mutual inclinations sampled, the resonant conditions are always fulfilled.

4. DISCUSSION

Our analysis continues to show that the non-Keplerian interaction between the two planets in the GJ 876 system indicates that the planets are participating in both the 2:1 mean motion resonances, as well as in the secular apsidal resonance. Radial velocities accumulated over the last 4 yr show that the libration widths of all three resonances are narrow, which argues for a dissipative history of differential migration for the system.

It is interesting to note, however, that the planet-planet interactions are in a sense quite subtle and suffer from a degeneracy that prevents simultaneously accurate measurement of the eccentricity of the inner planet and the overall inclination of the system. Extensive Monte Carlo simulations suggest that the eccentricity of the inner planet lies in the range $0.2 < e_c < 0.35$ and that the system has $i_s > 20°$. This situation is based on an assumption for the stellar jitter of 6 m s^{-1}. If this assumption turns out to be conservative and the actual jitter is less, then it will be possible to obtain considerably better constraints on the orbital parameters of the system, and as more radial velocities are obtained, perhaps confirm or rule out the presence of additional small bodies in this remarkable exoplanetary system.

Plausible and detailed histories for the origin of the resonances in the GJ 876 system were proposed by Lee & Peale

(2001, 2002). In their scenario, the planets originally formed in low-eccentricity orbits with semimajor axes larger than those currently observed and with a larger period ratio than the present-day 2:1 commensurability. The planets then grew large enough to open gaps in the protoplanetary disk. Hydrodynamic simulations by Bryden et al. (2000) and Kley (2000) suggest that a residual ring of disk material between two massive planets is rapidly cleared as a consequence of repeated spiral shock passages from the protoplanetary wakes. This clearing process appears to require only several hundred orbits after the planets have been established. After the ring of gas between the planets has vanished, the planets will experience differential migration. The spiral wake driven through the outer disk will exert a negative torque on the outer planet, causing it to spiral inward. The inner planet will either be pushed outward by a remnant inner disk, or more likely, retain a more or less constant semimajor axis. The inward-migrating outer planet then captures the inner planet into a low-order mean motion resonance (which in the case of GJ 876 was the 2:1), and the planets migrate in together. Lee & Peale (2002) demonstrated this mode of resonant capture for GJ 876 through the use of torqued three-body simulations. Additional *N*-body simulations of the GJ 876 precursor system were performed by a number of authors, including Snellgrove et al. (2001), Murray et al. (2002), Nelson & Papaloizou (2002), and Beaugé et al. (2004). More recently, full hydrodynamical simulations by Papaloizou (2003) and Kley et al. (2004) have also demonstrated capture of GJ 876 b and c into the observed resonances

as a consequence of differential migration driven by disk torques.

Once the planets are migrating in resonance in response to outer disk torques, the orbits lose angular momentum and energy at different rates. In the absence of a dissipative mechanism, this mismatch causes the planetary eccentricities to increase. Lee & Peale (2002) introduced an ad hoc eccentricity damping term to the migration. In cases where eccentricity damping was not used, they found that the semimajor axes decreased by only 7% before the eccentricities were pumped to their observed nominal values ($e_c = 0.22$, and $e_b = 0.03$). They therefore suggested that either (1) the disk dissipated before the planets were able to migrate very far, or alternately, (2) an effective mechanism exists for eccentricity damping during resonant migration.

Option 1 appears to require fine-tuning in order to provide an explanation for the current state of the GJ 876 system. The GJ 876 red dwarf, with $M = 0.3\,M_\odot$, is nearly 100 times less luminous than the Sun. The inner planet, GJ 876 c, with its surface temperature $T \sim 210$ K, is not far inside the location of the current snow line of the GJ 876 system. For GJ 876 b, located at $a = 0.2$ AU, we estimate a temperature at $\tau = 1$ of $T_b \sim 160$ K, which places it at or beyond the present snowline. The stellar evolution models of Baraffe et al. (2002), however, indicate that during contraction phases between 1 and 10 million years when giant planet formation likely took place, GJ 876 was more than 10 times as luminous as it is now. The possibility of nearly in situ formation for the GJ 876 planets is therefore unlikely but not fully out of the question (see, e.g., the accretion models of Bodenheimer et al. 2000). Certainly, the comparatively luminous early phases of M star evolution pose interesting tests for theories of planet formation.

Option 2 may also be problematic. Recent two-dimensional hydrodynamic simulations, such as those of Kley et al. (2004) are able to follow the planet/planet-disk evolution over secular timescales $t > 5\times 10^4$ yr. These simulations self-consistently model both the resonance capture and differential migration processes and show that eccentricity damping arising from the disk gas is much smaller than that required by Lee & Peale (2002) to explain the current state of the GJ 876 system as arising from significant differential migration. Kley et al. (2004) remark, however, that it remains to be seen whether three-dimensional hydrodynamic calculations, which incorporate a more realistic equation of state and which adequately resolve the gas flow close to the planets, will provide the needed increase in the eccentricity damping rate.

The low expected temperature of GJ 876 c leads naturally to speculation that a potentially habitable terrestrial world might exist in the system. The usual definition of the planetary habitability zone, as given in Kasting et al. (1993), combined with the stellar properties of GJ 876, suggests that the habitable zone of GJ 876 is located interior to the orbit of planet c

($a_c = 0.13$ AU) at a radius $r_h \sim 0.1$ AU. Menou & Tabachnik (2003) report that terrestrial planets placed in habitable circular orbits with 0.1 AU $< a < 0.2$ AU are rapidly ejected by the outer two planets. We have verified this conclusion using the updated orbital parameters given in Table 2.

We remark, however, that the clear history of resonant capture and inward dynamical migration in this system suggests that a terrestrial-mass object orbiting interior to the two gas giant planets may have been captured into a 2:1 resonant orbit with GJ 876 c, leading to a high-eccentricity analog of the Laplacian resonant condition observed among Io, Europa, and Ganymede. Such an object would have an orbital period of order $P \sim 15$ days and a semimajor axis of $a_t = 0.08$ AU. Numerical experiments show that stable systems of this sort are readily found in which the resonant argument θ_2 between the planet c and the putative interior terrestrial planet is librating, and where the eccentricity of the terrestrial planet is $e_t \sim 0.3$. If such a system is not fully coplanar, then one can expect precession of the nodal line, and hence periodically recurring transits. An Earth-size planet transiting GJ 876 would produce a transit depth of 0.3%, which is readily detectable with modest-aperture telescopes from the ground (Henry 1999). A habitable planet in the GJ 876 system would display a maximum separation from the primary star of approximately 20 mas, which places the system within the top 300 candidates among the 1139 nearby stars currently being considered as potential targets for NASA's *TPF* mission.[6]

It is likely that the GJ 876 system will reveal further surprises as it is studied photometrically and spectroscopically from the ground and from space. Furthermore, even the present radial velocity data set may harbor much additional information if the stellar jitter turns out to be smaller than $\sigma = 6$ m s^{-1} that we have assumed in this study.

[6] See the TPF target list at http://planetquest.jpl.nasa.gov/Navigator/library/basdtp.pdf.

REFERENCES

Baraffe, I., Chabrier, G., Allard, F., & Hauschildt, P. H. 2002, A&A, 382, 563
Beaugé, C., Ferraz-Mello, S., & Mitchtchenko, T. A. 2004, MNRAS, in press
Benedict, G. F., et al. 2002, ApJ, 581, L115
Binzel, R. P. 1989, Geophys. Res. Lett., 16, 1205
Bodenheimer, P., Hubickyj, O., & Lissauer, J. L. 2000, Icarus, 143, 2
Bodenheimer, P., Laughlin, G., & Lin, D. N. C. 2003, ApJ, 592, 555
Bryden, G., Rozyczka, M., Lin, D. N. C., & Bodenheimer, P. 2000, ApJ, 540, 1091
Delfosse, X., Forveille, T., Mayor, M., Perrier, C., Naef, D., & Queloz, D. 1998, A&A, 338, L67
Ford, E. 2003, preprint (astro-ph/0305441)

Goldreich, P., & Soter, S. 1966, Icarus, 5, 375
Guillot, T., & Showman, A. P. 2002, A&A, 385, 156
Henry, G. 1999, PASP, 111, 845
Henry, T. J., & McCarthy, D. W. 1993, AJ, 106, 773
Kasting, J. F., Whitmire, D. P., & Reynolds, R. T. 1993, Icarus, 101, 108
Kley, W. 2000, MNRAS, 313, L47
Kley, W., Peitz, J., & Bryden, G. 2004, A&A, 414, 735
Konacki, M., & Wolszczan, A. 2003, ApJ, 591, L147
Laplace, P. S. 1799–1802, Traité de Mécanique Céleste, Volumes 1–3 (Paris: Duprat)
Laughlin, G., & Chambers, J. E. 2001, ApJ, 551, L109

Lee, M. H. 2004, ApJ, 611, 517
Lee, M. H., & Peale, S. J. 2001, BAAS, 33, 1198
———. 2002, ApJ, 567, 596
———. 2003, ApJ, 592, 1201
Marcy, G. W., Butler, R. P., Fischer, D., Vogt, S. S., Lissauer, J. J., & Rivera, E. J. 2001, ApJ, 556, 396
Marcy, G. W., Butler, R. P., Vogt, S. S., Fischer, D. A., & Lissauer, J. J. 1998, ApJ, 505, L147
Menou, K., & Tabachnik, S. 2003, ApJ, 583, 473
Murray, N., Paskowitz, M., & Holman, M. 2002, ApJ, 565, 608
Nauenberg, M. 2002, AJ, 124, 2332
Nelson, R. P., & Papaloizou, J. C. B. 2002, MNRAS, 333, L26

Papaloizou, J. C. B. 2003, Celest. Mech. Dyn. Astron., 87, 53
Perryman, M. A. C., et al. 1997, A&A, 323, L49
Press, W. H., Teukolsky, S. A., Vetterling, W. T., & Flannery, B. P. 1992, Numerical Recipes: The Art of Scientific Computing (2nd ed.; Cambridge: Cambridge Univ. Press)
Rivera, E. J., & Lissauer, J. J. 2001, ApJ, 558, 392
Saar, S. H., Butler, R. P., & Marcy, G. W. 1998, ApJ, 498, L153
Seagroves, S., Harker, J., Laughlin, G., Lacy, J., & Castellano, T. 2003, PASP, 115, 1355
Snellgrove, M. D., Papaloizou, J. C. B., & Nelson, R. P. 2001, A&A, 374, 1092
Thommes, E. W., & Lissauer, J. J. 2003, ApJ, 597, 566
Wolszczan, A., & Frail, D. A. 1992, Nature, 355, 145